Ecological Complexity 20 (2014) 315–324

Contents lists available at ScienceDirect

Ecological Complexity

journal homepage: www.elsevier.com/locate/ecocom

Original Research Article

Extrapolation methods for climate time series revisited – Spatial correlations in climatic fluctuations influence simulated tree species abundance and migration

Julia E.M.S. Nabel [a,b,*], James W. Kirchner [b], Natalie Zurbriggen [a], Felix Kienast [a], Heike Lischke [a]

[a] Landscape Dynamics, Swiss Federal Institute for Forest, Snow and Landscape Research WSL, Zürcherstrasse 111, 8903 Birmensdorf, Switzerland
[b] Department of Environmental Systems Science, Swiss Federal Institute of Technology ETH, Universitätstrasse 16, 8092 Zürich, Switzerland

ARTICLE INFO

Article history:
Received 13 July 2013
Received in revised form 19 January 2014
Accepted 21 February 2014
Available online 27 March 2014

Keywords:
Spatially correlated climatic fluctuations
Interannual climate variability
Spatially explicit
Spatially linked
Tree species migration
TreeMig

ABSTRACT

Simulations of tree population dynamics under past and future climatic changes with time- and space-discrete models often suffer from a lack of detailed long-term climate time series that are required to drive these models. Inter- and extrapolation methods which are applied to generate long-term series differ in terms of whether they do or do not account for spatial correlation of climatic fluctuations. In this study we compared tree species abundance and migration outcomes from simulations using extrapolation methods generating spatially correlated (SC) and spatially independent (SI) climatic fluctuations. We used the spatially explicit and linked forest-landscape model TreeMig and a simple cellular automaton to demonstrate that spatial correlation of climatic fluctuations affects simulation outcomes. We conclude that methods to generate long-term climate time series should account for the spatial correlation of climatic fluctuations found in available climate records when simulating tree species abundance and migration.

1. Introduction

Climate is regarded as the main determinant of species ranges on broad geographical scales (Pearson and Dawson, 2003; Rosenzweig et al., 2007; Normand et al., 2011). Many processes in the life cycle of plants, such as growth, survival and reproduction, are affected by climatic conditions, whereby long-term trends as well as climatic fluctuations are influential (Brubaker, 1986; Laakso et al., 2001; Jackson et al., 2009). Climatic changes induce changes of ecosystems, including shifts of species ranges and changes in species compositions (Lyford et al., 2003; Rosenzweig et al., 2007; Midgley et al., 2007). These changes, however, seldom occur abruptly but rather slowly, and especially long-lived ecosystems such as forests show lag effects in their reactions to climatic changes because of the slow nature of tree population dynamics (Pitelka et al., 1997; Fischlin et al., 2007; Sato and Ise, 2012). Therefore, simulations of such ecosystems need to be conducted for long time spans.

Tree population dynamics under past and future climatic changes are often studied with time- and space-discrete models. Studies range from simulations of single sites (e.g. Bugmann, 2001; Giesecke et al., 2010) to spatially explicit simulations with and without spatial linkage of the simulated grid cells (e.g. Lischke et al., 2013; Hickler et al., 2012). One of the main problems of simulation studies for long time spans is the availability of climate data. For simulations of the past often only proxy data for sparse points in time is available, for example from lake sediments or tree rings. From such proxy data climate anomalies can be derived, ranging from 1000-year time periods (e.g. Miller et al., 2008; Giesecke et al., 2010) or approximately 250-year time periods (e.g. Lischke, 2005) to, at the best, around 10 to 20-year time periods (e.g. Lischke et al., 2013). Thus, they miss crucial short-term fluctuations. For simulations of the future, detailed climate projections often only reach until 2100, which is not sufficient to study slow tree population dynamics (Bugmann, 2001; Hickler et al., 2012), especially not trends in tree species migration (Nabel et al., 2013).

Generally, to obtain long-term climate drivers with daily, monthly or yearly resolution, past and future climate time series

* Corresponding author at: Present address: Max Planck Institute for Meteorology, Bundesstrasse 53, 20146 Hamburg, Germany. Tel.: +49 40 41173 260; fax: +49 40 41173 298.
E-mail address: jemsnabel@gmail.com (Julia E.M.S. Nabel).

http://dx.doi.org/10.1016/j.ecocom.2014.02.006
1476-945X/

often need to be interpolated or extrapolated. Due to the influence of climate variability on tree population dynamics, the most simplistic approaches, such as linear interpolation, or extrapolation by steadily applying mean values, are not appropriate (Giesecke et al., 2010; Nabel et al., 2013). More sophisticated inter- and extrapolation methods use selected base periods of available climate time series to generate climatic fluctuations. Such methods can directly use the 'empirical distribution' given by the climatic fluctuations that are actually observed in the base years or can sample from probability distributions derived from the statistical properties of the base years. Concordantly, Bugmann (2001) listed three methods applied in forest gap models to extrapolate climatic conditions, namely (1) cyclically repeating available records, (2) randomly selecting from available records and (3) generating random series based on probability distributions derived from available records. Bugmann (2001) recommended the third approach for the application with forest gap models. This approach also has been used in various simulations with the spatially explicit and linked forest-landscape model TreeMig (see e.g. Lischke, 2005; Epstein et al., 2007; Lischke et al., 2013; Nabel et al., 2013). In these TreeMig simulations climatic fluctuations were sampled independently for each single cell of the simulated area.

Whilst sampling from probability distributions might be recommended for forest gap models, which simulate single stands, we question whether it is suitable for models, such as TreeMig, that simulate a landscape of spatially explicit and linked cells. When sampling climatic fluctuations independently for each cell of a landscape, the spatial correlation in the climatic fluctuations among cells is lost and we hypothesise that this eventually could influence spatial correlations of simulated population dynamics. However, biological processes do not necessarily respond linearly to climate drivers (Laakso et al., 2001) and spatial correlation in climatic fluctuations therefore does not automatically have to translate into spatially correlated biotic responses, particularly not in spatially heterogeneous environments (Grenfell et al., 2000; Greenman and Benton, 2001; Currie, 2007). Nevertheless, many studies found that synchronous climatic fluctuations can lead to synchronisations in population dynamics of various (animal and plant) taxa (Koenig, 2002; Liebhold et al., 2004). Examples for observed synchronised events in tree population dynamics attributed to spatial correlations in fluctuations of climatic drivers are synchronised masting behaviour (Koenig and Knops, 2013), pulses of range expansion in favourable years (Lyford et al., 2003; Jackson et al., 2009) and synchronised mortality events in unfavourable years (Breshears et al., 2005). Sampling random fluctuations independently for each cell of a simulation area in order to inter- or extrapolate a climate driver removes such potential synchronisations and we hypothesise that this will affect simulated tree species abundance and migration. Studies on invasive species already demonstrated the importance of climatic fluctuations and of static spatial heterogeneity for migrating species (e.g. With, 2002; Hui et al., 2011). However, the combination, i.e. spatiotemporal heterogeneity (sensu Melbourne et al., 2007), has so far not been well studied (With, 2002; Melbourne et al., 2007; Hui et al., 2011). Furthermore, results of previous studies on the influence of static spatial heterogeneity are not simply transferable to the case studied here, because neglecting the spatial correlation in the fluctuations of a climate driver does not disturb the underlying spatial heterogeneity given by the mean of the climate driver.

In summary, the overall research questions are whether neglecting spatial correlation in climatic fluctuations (1) leads to a loss in the synchronisation of species abundances and (2) affects simulated tree species migration.

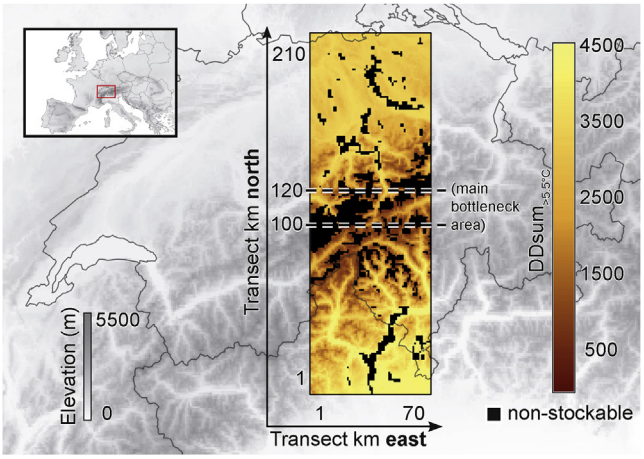

Fig. 1. Transect through the climatically heterogeneous and fragmented landscape of the Swiss Alps (210 km × 70 km; grid-cell size 1 km^2). Background: digital elevation model from Jarvis et al. (2008). Colour-gradient: mean value of one of TreeMigs bioclimate variables – the $DDsum_{>5.5°C}$ (sum of daily mean temperatures above 5.5 °C) for the simulation years 2071–2100 (see Section 2.1.3). In this study, the shown transect was used as simulation area in applications of the model TreeMig. Black cells represent cells where trees cannot grow (non-stockable in TreeMig), here: solid rock surfaces and large water bodies. The area between the dashed lines (100th to 120th transect km north) approximately corresponds to the main bottleneck area of the transect.

In this study, we used the intermediate-complexity forest-landscape model TreeMig to test for effects of spatial correlation in climatic fluctuations on tree species abundance and migration outcomes. These tests were conducted with an illustrative example setup, simulating the northwards migration of a sub-Mediterranean tree species on a transect through the Swiss Alps (Fig. 1). This example was selected because it proved to be sensitive to different realisations of TreeMigs bioclimate drivers in previous studies (Nabel et al., 2012, 2013). The large number of interacting processes and species parameters in TreeMig (see Lischke et al., 2006) hampers a detailed analysis of the influence of spatial correlation in bioclimatic fluctuations on tree species migration. Therefore, we additionally developed a simple individual-based cellular automaton focussing on the first steps required for tree species migration, namely availability of seeds (linked to the presence of adults), germination and survival to maturity. Germination and survival to maturity are critical steps, since juveniles are often more susceptible to climatic influences than adults (Lyford et al., 2003; Jackson et al., 2009). Furthermore, these first steps were the primary bottleneck for migration in previous TreeMig simulations of the illustrative example setup (Nabel et al., 2013).

2. Methods

2.1. TreeMig

TreeMig is a multi-species, spatially linked and dynamic intermediate-complexity model simulating forest landscapes (Lischke et al., 2006). TreeMig's state variables are height-structured population densities per species. Local stand dynamics are represented by seed-bank dynamics, germination, growth, death and seed production (Lischke et al., 2006; Lischke and Löffler, 2006). The spatial linkage among cells is realised via seed dispersal applying a deterministic dispersal kernel composed of two negative exponentials that are parameterised according to dispersal properties of the simulated species (Lischke and Löffler, 2006). TreeMig accounts for inter- and intra-specific competition for light by modulating the local stand dynamics according to light

Table 1
Influence of the three bioclimate variables used in TreeMig on TreeMig's processes. All listed processes are additionally influenced by inter-specific competition. For a detailed documentation of TreeMig's processes see (Lischke et al., 2006).

	$DDsum_{>5.5°C}$[a]	*Min. WiTemp*[b]	*Drought severity*
Germination	Threshold, absolute	Threshold, absolute	–
Mortality	Threshold, multiplicative thinning effect	–	Threshold, multiplicative thinning effect
Growth	Asymptotic	–	Linear decay with threshold

[a] Sum of daily mean temperatures above 5.5 °C.
[b] Minimum winter-temperature.

availability (Lischke et al., 2006). Due to the represented processes, TreeMig has the rare advantage of simultaneously allowing for explicit simulation of tree species migration and of inter-specific competition (Lischke et al., 2006; Nabel et al., 2013).

2.1.1. Influence of bioclimate variables in TreeMig

TreeMig simulations are driven by three annual bioclimate variables: the sum of daily mean temperatures above 5.5 °C ($DDsum_{>5.5°C}$), the minimum winter temperature (*Min. WiTemp*) and an index representing the severity of drought events (*Drought severity*). These bioclimate variables were derived from observed (1901–2000) and projected (2001–2100) monthly climate data. $DDsum_{>5.5°C}$ and *Min. WiTemp* were derived from monthly average temperatures and *Drought severity* from monthly average temperatures, monthly precipitation sums, water storage capacity as well as slope and aspect of each simulation cell. A detailed description and data sources are given in the electronic supplementary material (ESM). The three bioclimate variables influence different TreeMig processes (see Table 1). For successful germination *Min. WiTemp* and $DDsum_{>5.5°C}$ need to exceed a species-specific threshold. The maximum possible annual growth of a species is asymptotically influenced by $DDsum_{>5.5°C}$ (Rickebusch et al., 2007) and decays as a function of *Drought severity* (Lischke et al., 2006). Mortality is directly influenced when $DDsum_{>5.5°C}$ or *Drought severity* exceed a species-specific threshold and indirectly influenced when growth is depleted (Lischke et al., 2006).

2.1.2. Methods to extrapolate TreeMig's bioclimate drivers

In previous TreeMig versions, bioclimate time series were inter- or extrapolated by sampling the bioclimate for each year and each cell independently from probability distributions (Lischke et al., 2006). These probability distributions were derived from a selected base period (see e.g. Lischke, 2005; Epstein et al., 2007; Lischke et al., 2013). Thereby the $DDsum_{>5.5°C}$, for example, was approximated with an independent normal distribution for each cell of the simulation area (see e.g. Lischke et al., 2006; Nabel et al., 2013). For this study TreeMig (**TreeMig-Netcdf 2.0**) was equipped with two additional methods, which both sample uniformly from

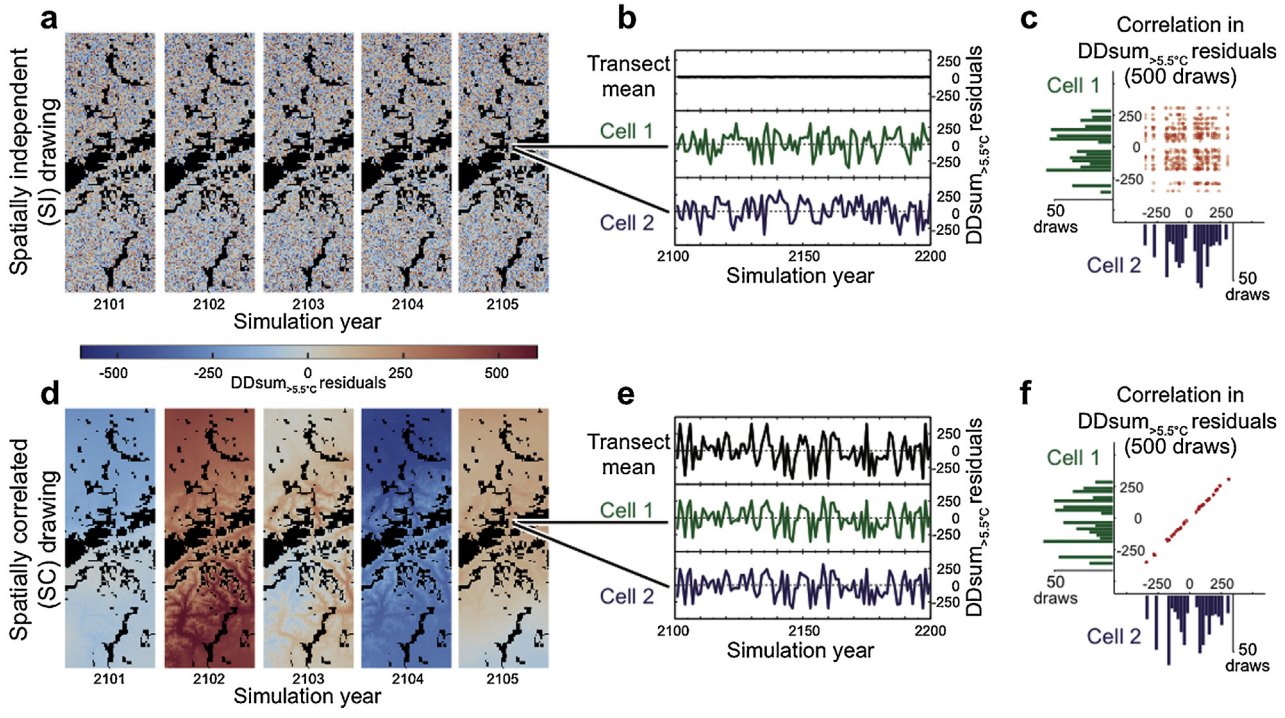

Fig. 2. Comparison of the applied extrapolation methods on the example of the bioclimate variable $DDsum_{>5.5°C}$. With the first method – spatially independent (SI) drawing – the bioclimate in a year is sampled independently for each cell of the simulation area. With the second method – spatially correlated (SC) drawing – a complete bioclimate map is drawn each year from the base years, i.e. the spatial arrangements and therefore the spatial correlation of the bioclimate found in the drawn base year is directly carried over. The two methods result in dramatic differences in the spatial arrangements of the deviation from the mean of the base years, as illustrated with the five generated $DDsum_{>5.5°C}$ maps (panel a: SI, panel d: SC) for the transect through the Swiss Alps (see Fig. 1). $DDsum_{>5.5°C}$ time series for single cells have comparable distributions, however, their correlation is disrupted for SI drawing (see time series in panel b compared to e and scatter plot with half-transparent markers and histograms in panel c compared to f). The average residuals over all transect cells resulting from simulations with SI drawing are always close to zero (panel b) because the random fluctuations drawn for the single cells tend to cancel each other out. For SC drawing, on the other hand, the average residuals over all transect cells reflect the interannual variability found in the base years.

the empirical distribution found in the base period, i.e. from the bioclimatic values that actually occur in the base years.

Spatially independent drawing (SI). With this method, the bioclimate of a year is sampled independently from the empirical distribution found in the base years for each cell, i.e. for each cell one base year is drawn (Fig. 2a). This base year is used for all bioclimate variables in the cell.

Spatially correlated drawing (SC). When selecting this method, a complete bioclimate map is drawn each year from the base-year set and its values are used for all cells of the simulation area (Fig. 2d) and all bioclimate variables.

SI drawing is a simplification of drawing from probability distributions because sampling from probability distributions also allows values outside of the range of the empirical distribution, i.e. outside of the range of the values that actually occur in the base years (Bugmann, 2001). We introduced this simplification to exclude effects solely caused by extreme values, which were not contained in the empirical distribution but were possible when drawing from derived probability distributions. Such effects could else have interfered with effects of spatial correlation in the bioclimate variables when comparing the simulation results for different extrapolation methods.

2.1.3. TreeMig simulation setup

The effects of spatially correlated fluctuations in TreeMig's bioclimate drivers on simulated species abundance and migration were studied with an illustrative example. We simulated the northwards migration of the sub-Mediterranean tree species *Ostrya carpinifolia* Scop. (European Hop Hornbeam) in a warming climate on a 210 km × 70 km simulation transect (grid-cell size of 1 km^2) through the Swiss Alps (Fig. 1). This example was chosen because it proved to be sensitive to different realisations of the bioclimate time series in previous simulation studies (Nabel et al., 2012, 2013).

For this study, outcomes of simulations applying the two bioclimate extrapolation methods SC and SI were compared. Simulations with SI and SC extrapolation started in the simulation year 2100 from the same model state, i.e. with the same values in the state variables, and used the same set of bioclimate base years (2071–2100). The generation of the bioclimate base-year set and the model state in 2100 follow the simulation setup as described by Nabel et al. (2013) (summarised in ESM A). The climate time series used to derive the bioclimate driver showed no consistent signal of temporal autocorrelation (see ESM A.1.3). Therefore, temporal autocorrelation was not examined in this study, although its influence on population dynamics has been widely discussed (e.g. Schreiber and Ryan, 2011; van de Pol et al., 2011).

Simulations were run up to the year 3000 and 100 repetitions were conducted for each of the two extrapolation methods and for two different species parameter sets for the focal species. These two species parameter sets represent the moderate to optimistic range of plausible species parameters for *O. carpinifolia* (see ESM A.2) and were selected because they resulted in a successful migration through the simulation transect in a previous study (Nabel et al., 2013).

In each simulation we tracked the biomass of *O. carpinifolia* and the sum of the biomass of all simulated species (see ESM A.2). For each cell of the simulation area these output variables were recorded per century, and their annual development was only tracked for selected single cells and as a sum over the entire transect. As an indicator for the spread of *O. carpinifolia* we recorded the annual development of its northernmost occurrence (NO in transect km – counted from the southernmost point of the transect), i.e. its momentary spread distance. In this paper, figures with maps of the transect were created with Paraview (Ahrens et al., 2005) and graphs with Matlab 11.

2.2. Cellular automaton

2.2.1. Structure of the cellular automaton

For this study we developed a single-species cellular automaton (CA). Each cell of the CA can be regarded as an abstract representation of one individual or one small stand of same-aged individuals of the focal species. A cell can be in one of three states: **empty**, **juvenile** or **mature** (Fig. 3).

In TreeMig, germination presupposes that bioclimate influences exceed certain species-specific thresholds (Table 1). Therefore, in the CA, a cell i changes from empty to juvenile only when the environmental conditions ($\mathbf{env}_i$ drawn from a normal distribution with mean 0 and standard deviation σ) exceed a specified germination threshold (g_{thresh}). Additionally, the number of seed providing sources for cell i ($\mathbf{seedsources}_i$), i.e. the number of mature cells in the simulated neighbourhood (*neighbourhood* – Fig. 3b), needs to exceed a threshold (s_{thresh}). Thus, the parameter s_{thresh} controls the incidence and the strength of positive density dependency. Moreover, because cells in the CA do not differ in terms of size, age or fitness, they also do not differ in the number of seeds they produce. Thus, the number of seed providing sources alone is used as a proxy for propagule pressure.

Transition from juvenile to mature happens when the age ($\mathbf{age}_i$) of the cell exceeds age_{mat}, i.e. when the individual survived in the state juvenile for this number of iterations. If the environmental conditions ($\mathbf{env}_i$) fall below the mortality threshold (m_{thresh}) while the cell is in the state juvenile its state changes back to empty. After reaching the mature state, a cell stays in this state for the rest of the simulation time and can provide seeds to cells in the simulated *neighbourhood* (Fig. 3b). Mortality was implemented not to affect mature individuals, because mortality for adults would have required an independent environmental threshold, since juveniles and adults often have different sensitivities to climatic influences (Lyford et al., 2003; Jackson et al., 2009). Furthermore, for migration, the development on the range limits is anyway more important than population fluctuations (i.e. mortality of adults) in parts of the simulation area far from the front (Melbourne et al., 2007).

In summary, the CA incorporates stochasticity for transitions between empty and juvenile (germination and mortality). The fluctuating environmental influence is implemented as a normal

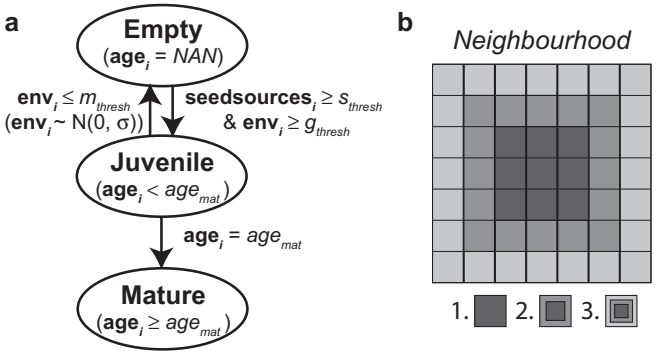

Fig. 3. Schematic of the cellular automaton (CA). Each cell of the CA can be in one of three different states: empty, juvenile and mature (panel a). A transition from empty to juvenile has two prerequisites: (1) the number of seed providing sources $\mathbf{seedsources}_i$, i.e. the number of mature cells in the selected *neighbourhood* (panel b), needs to exceed the threshold s_{thresh} and (2) the environmental conditions $\mathbf{env}_i$, which are drawn from a normal distribution with mean 0 and standard deviation σ, need to exceed the germination threshold g_{thresh}. If the environmental conditions $\mathbf{env}_i$ fall below the mortality threshold m_{thresh} while a cell is in the state juvenile its state changes back to empty. A transition from juvenile to mature happens when the age $\mathbf{age}_i$ of the cell exceeds age_{mat}. A mature cell stays mature for the rest of the simulation time. Simulations were conducted with three different neighbourhoods (panel b).

```
PROGRAM CA
SET age (age_i) for each cell to NAN
FOR each time step
    IF spatially correlated (SC) drawing
        CALL draw environment (env_i) for all cells
    END IF
    FOR each cell
        IF spatially independent (SI) drawing
            CALL draw environment (env_i) for this cell
        END IF
        IF age_i < age_mat AND env_i ≤ m_thresh
            SET age_i to NAN
        ELSEIF age_i == NAN AND env_i ≥ g_thresh
            SET seedsources_i to zero
            FOR each other cell j in neighbourhood
                IF age_j ≥ age_mat
                    INCREMENT seedsources_i
                END IF
            END FOR
            IF seedsources_i ≥ s_thresh
                SET age_i to zero
            END IF
        ELSEIF age_i ≠ NAN
            INCREMENT age_i
        END IF
    END FOR
END FOR
```

Fig. 4. Pseudocode of the cellular automaton. State variables are printed in bold, parameters in italic type.

distribution with mean 0 and standard deviation σ. The two different approaches to draw environmental influences were implemented such that in case of spatially correlated (SC) drawing only one pseudo-random number is drawn for the entire area, whilst in case of spatially independent (SI) drawing an independent pseudo-random number is drawn for each cell. A pseudocode of the CA is given in Fig. 4. A vectorised version of the CA was implemented in Matlab 11 (see ESM C).

2.2.2. CA simulation setup

In accordance with the TreeMig simulations, a northwards migration was simulated with the CA. Simulations were conducted on a grid with 50 cells in west-east and 200 cells in north-south direction with cyclic and absorbing boundary conditions, respectively. The lowest two rows were initialised with the state juvenile: $\mathbf{age}_i = 1 (i = 1, \ldots, 100)$. The mean environmental influence of all cells of the simulation area was assumed to be zero. In case of SC drawing the simulation area was thus spatially homogeneous and only fluctuated among iterations.

Simulations were conducted for different combinations of parameter values (Table 2). For both methods to draw environmental influences each combination was simulated with 100 repetitions (in total 480,000 runs). In each of 100 iteration steps the northernmost occurrence was tracked (in number of rows from the southernmost row including the lowest two rows).

3. Results

3.1. TreeMig simulations of tree species abundance

Despite the strong synchronisation of bioclimatic fluctuations (Fig. 2d–f), simulations with SC extrapolation only showed partial synchronisation of the simulated biomass, i.e. residuals of the same colour in Fig. 5c. However, where fluctuations of the biomass of *O. carpinifolia* were synchronised in simulations with SC extrapolation this synchronisation was disrupted in simulations with SI extrapolation (Fig. 5a). In addition to the maps shown in Fig. 5 we provide further analyses of biomass correlations over time for selected single cells in the ESM (Figs. B.1 and B.2).

The biomass sum of *O. carpinifolia* (Fig. 5b and d) over the whole transect showed similar effects to the transect mean of the bioclimate driver (Fig. 2b and e): for simulations with SI extrapolation the sums were nearly invariant over time and among realisations (Fig. 5b) – apart from the biomass increase of *O. carpinifolia* due to its northwards migration. For simulations with SC extrapolation, on the other hand, the biomass of *O. carpinifolia* varied greatly (20-55 kt – Fig. 5d). The same effects were observed for the sum of the biomass of all simulated species (see ESM Fig. B.3).

3.2. Simulations of tree species migration

3.2.1. Simulations with TreeMig

Northernmost occurrences among simulations with SI and SC extrapolation and among their repetitions (Fig. 6) diverged when *O. carpinifolia* entered the main bottleneck area (approximately at the 100th transect km north, Fig. 1). For both extrapolation methods, simulations with the moderate, less favourable parameter set for *O. carpinifolia* (Fig. 6b) resulted in slower migration rates and a higher variability in the northernmost occurrences among the 100 repetitions than simulations with the optimistic parameter set (Fig. 6a). In simulations with the optimistic parameter set, trajectories of the northernmost occurrence were almost parallel for all runs, i.e. they have the same migration speed, aside from two bottleneck situations (Fig. 6a).

The distributions of the northernmost occurrence in the simulation year 3000 resulting from repetitions with SC extrapolation and SI extrapolation are significantly different: for both species parameter sets, the year-3000 distribution mean for SI repetitions does not fall into the interquartile range of the distribution of SC repetitions (Fig. 6). SC repetitions showed a variability approximately 1.2-fold and 1.5-fold the variability of SI repetitions for the moderate parameter set and the optimistic parameter set, respectively.

Differences in the time points when *O. carpinifolia* passed the bottleneck situation of the simulation area led to large differences

Table 2
Parameters used for simulations with the cellular automaton and their function. The first five parameters are the species parameters of the focal species. The sixth parameter – σ – determines the variability of the environmental fluctuations.

	Parameter values	Function
age_{mat}	{1, 3, 5, 10}	Iterations after which a cell in the state juvenile changes to the state mature
g_{thresh}	{0, 1, 2, 3, 4}	Germination threshold ($\geq$: positive influence of environmental variability; small values (close to 0) imply frequent germination, large values infrequent germination)
m_{thresh}	{−4, −3, −2, −1, 0}	Mortality threshold ($\leq$: negative influence of environmental variability; small values (close to −4) imply infrequent deaths, large values frequent deaths)
s_{thresh}	{1, 3, 5, 10}	Determines the number of required seed sources to achieve a successful germination and therefore the incidence and the strength of positive density dependency
neighbourhood	{1, 2, 3}	Determines the neighbourhood that a mature cell provides seeds for (see Fig. 3b)
σ	{1, 2}	Standard deviation of the normal distribution used to represent environmental fluctuations (see Fig. B.5 in the ESM for example histograms)

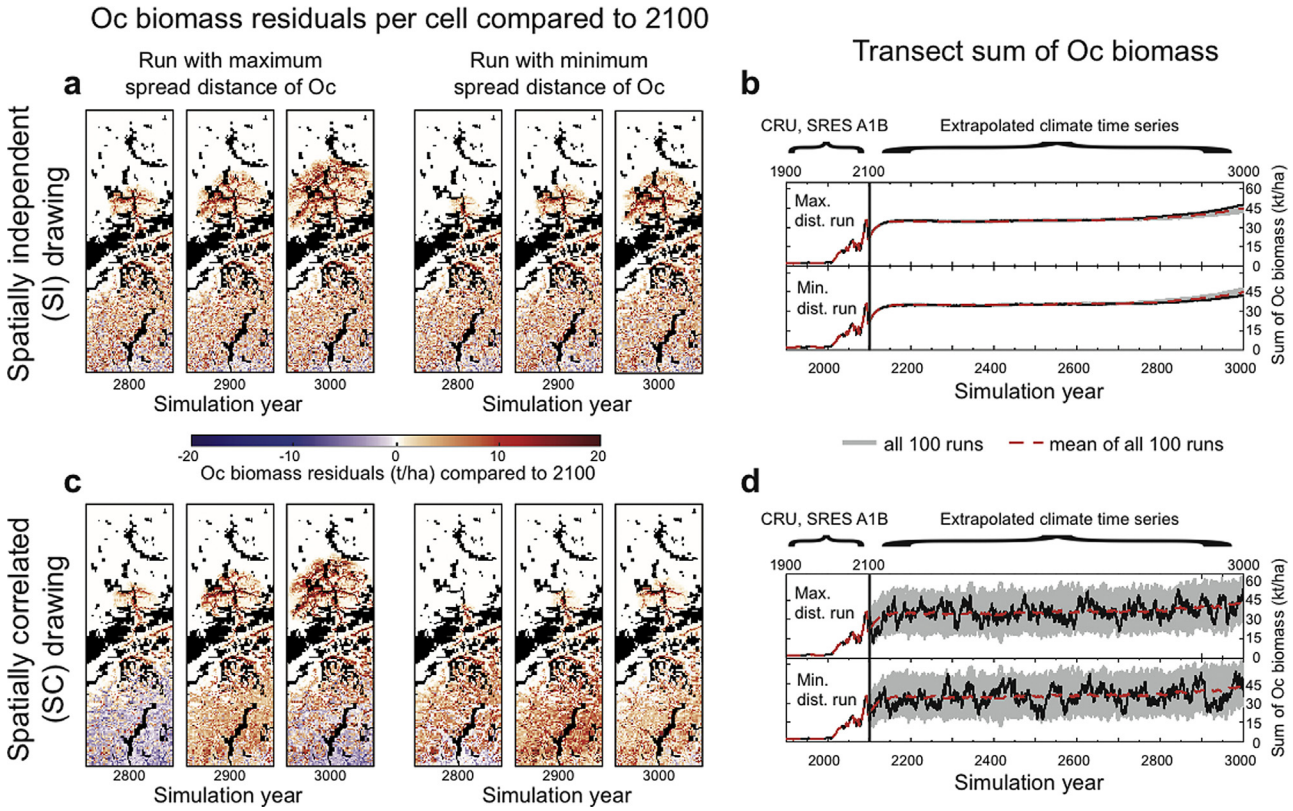

Fig. 5. Abundance of *O. carpinifolia* (Oc) resulting from TreeMig simulations for different runs with the two extrapolation methods: spatially independent (SI) and spatially correlated (SC) drawing and the optimistic parameter set for *O. carpinifolia*. Depicted are maps for the simulation years 2800, 2900 and 3000 of simulated biomass residuals (t/ha) after subtracting the biomass resulting for the year 2100, from when on the bioclimate time series were extrapolated. For both, SI (panel a) and SC drawing (panel c), maps show the run with the maximum and the run with the minimum spread distance of *O. carpinifolia* in the simulation year 3000, i.e. the runs in which *O. carpinifolia* expanded most and least, respectively. The maps from simulations with SC drawing show a synchronisation of species abundances (accumulation of negative (blue) or positive (red) residuals), as opposed to maps from simulations with SI drawing in which no synchronisation is visible. Discrepancy of SC-runs and SI-runs get particularly clear when comparing the transect sums of the simulated biomass for *O. carpinifolia* for 1900–3000. The transect sum resulting from SI-runs (panel b) is nearly invariant over time and among realisations. For SC-runs (panel d), by contrast, the transect sum shows much larger and more realistic variability over time and among realisations. Black lines show the run with the maximum and minimum spread distance, respectively. Grey lines in the background are results from all 100 runs and the dashed red line represents the running mean over these 100 runs. (For interpretation of the references to colour in this figure legend, the reader is referred to the web version of this article.)

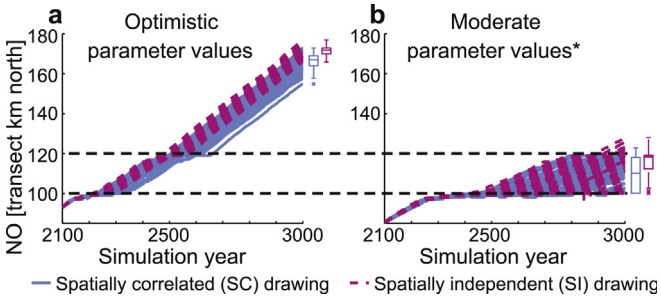

Fig. 6. Comparison of spread distances resulting from TreeMig simulations with spatially correlated (SC) and spatially independent (SI) drawing of bioclimate influences. Depicted are northernmost occurrences (NO in transect km north, smoothed over 10 years) in the simulation years 2100–3000 resulting from 100 repetitions with the two drawing methods and for two different species parameter sets for *O. carpinifolia*. (Panel a) Optimistic parameter values. (Panel b) Moderate parameter values (* with the optimistic parameter for the required $DDsum_{>5.5°C}$, see ESM A.2). The box plots on the right side of each panel depict the NO-distribution in the simulation year 3000 resulting from the 100 repetitions for each drawing method. For both parameter sets the NO in the simulation year 3000 show faster migration for and less variability among runs with SI drawing than with SC drawing. Box edges represent the interquartile range, whiskers extreme data points and crosses outliers. The black dashed lines mark the main bottleneck area of the transect (see Fig. 1).

in the spatial spread of *O. carpinifolia*. Differences between the runs with the maximum and the minimum spread distances in the simulation year 3000, for example, are much smaller in simulations with SI than with SC drawing (e.g. compare differences between SI maps in panel a and SC maps in panel c in Fig. 5).

3.2.2. Simulations with the CA

Whether the migration speed was higher in runs with SC or SI drawn environmental influences in the CA simulations depended on the species parameter values (see e.g. Fig. 7). For most of the simulated parameter sets the simulated migration was on average faster in runs with SI than in runs with SC drawn environmental influences (for summary statistics of all simulated parameter combinations see Table B.1 in the ESM). Only for some of the parameter sets with a positive density dependence ($s_{thresh} > 1$) and small to intermediate neighbourhood (*neighbourhood* 1 or 2) migration was on average slower for SI-runs (see e.g. Fig. 7c). In situations with minor environmental constraints (m_{thresh} close to −4 and g_{thresh} close to 0) migration speed for good dispersers (*neighbourhood* 2 or 3) was on average equal in SC- and SI-runs (see e.g. Fig. 8). Overall, variations in the environmental thresholds led to comparable effects among simulations with SI and SC drawing (Fig. 8 and ESM B.2.3).

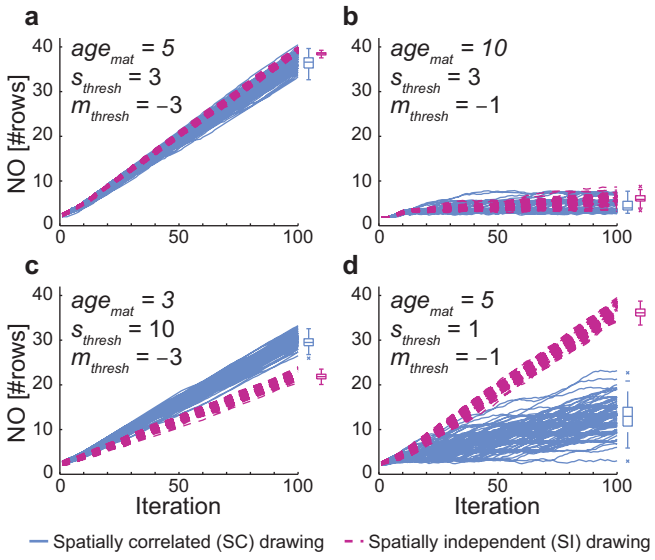

Fig. 7. Comparison of spread distances resulting from simulations with the cellular automaton (CA), with spatially correlated (SC) and spatially independent (SI) drawing of environmental influences. Depicted are northernmost occurrences (NO in number of rows, smoothed over ten iterations) resulting from 100 repetitions for each of the two drawing methods and four different parameter sets. The four parameter sets differ in the applied values for the age of maturity (age_{mat}), the required number of seed sources (s_{thresh}) and the mortality threshold (m_{thresh}). All parameter sets were simulated with germination threshold $g_{thresh} = 0$, *neighbourhood* 2 (Fig. 3) and standard deviation $\sigma = 1$. The first two parameter sets (panel a, b) were selected because their migration outcomes visually resemble the TreeMig outcomes for simulations of the migration of *O. carpinifolia* (Fig. 6). The two other parameter sets (panel c, d) show examples for the range of possible results within the simulated parameters (Table 2). The box plots on the right side of each panel depict the distributions of northernmost occurrences resulting from the 100 repetitions in the 100th iteration for each of the two extrapolation methods. Box edges represent the interquartile range, whiskers extreme data points and crosses outliers.

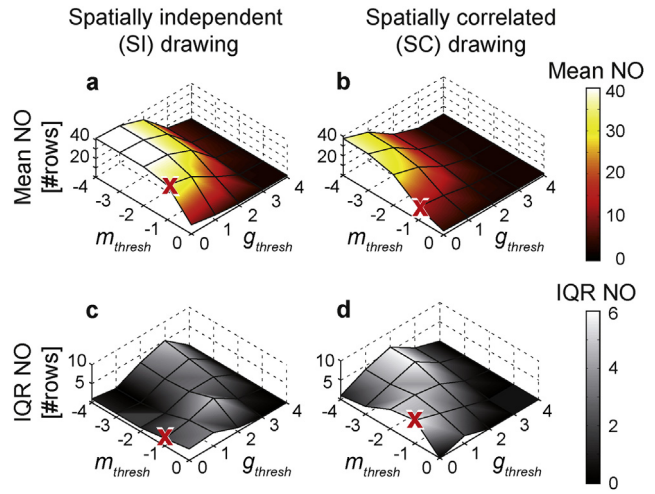

Fig. 8. Mean and interquartile range (IQR) of the northernmost occurrences (NO in number of rows) in applications of the cellular automaton as a function of all values simulated for the mortality threshold (m_{thresh}) and the germination threshold (g_{thresh}). Depicted are the mean (panel a and b) and the IQR (panel c and d) of the NO in the 100th iteration, calculated from 100 repetitions with *neighbourhood* 2 (Fig. 3), maturity age $age_{mat} = 5$, required number of seed sources $s_{thresh} = 1$ and standard deviation $\sigma = 1$ for the spatially independent (SI, panel a and c) and the spatially correlated (SC, panel b and d) drawing. The red crosses in the surface plots depict the parameter combination shown in Fig. 7d.

Whilst the number of required seed sources (s_{thresh}) had a strong effect on simulations with SI drawn environmental influences, this parameter had weaker effects on SC-runs (e.g. compare Fig. 7a with Fig. 7c). This is intuitive, because in SC-runs the environment in each iteration is the same for all cells and, therefore, same-aged cells are perfectly synchronised. Thus, if a row contains one mature cell, then all cells in this row are mature (see the ESM for a visualisation example).

For many parameter sets the variability in spread distances among SI-runs was very low and, in particular, for most simulated parameter sets lower than among SC-runs (see Fig. 7, Fig. 8 and ESM B.2).

4. Discussion

The results of the presented TreeMig simulations confirmed that tree species abundance and migration outcomes are influenced by the spatial correlation of climatic fluctuations. Simulations with the simple cellular automaton, furthermore, affirmed that the different methods to generate fluctuations in the model driver can lead to large differences in migration speed and variability among runs with the same set of species parameters.

4.1. Simulated tree species abundance

The ubiquitous synchronism of the fluctuations in the bioclimate driver in TreeMig simulations with SC extrapolation (Fig. 2) did not lead to an equally ubiquitous synchronism in simulated tree species abundances (Fig. 5). This was expected, because the synchronised fluctuations are only superimposed on the spatially heterogeneous mean bioclimate influences (Fig. 1). As already stated in the introduction, this underlying spatial heterogeneity is very important, because population dynamics – in models like TreeMig and in natural systems – can be non-linear (Laakso et al., 2001). Thus, the synchronised fluctuations in the driver do not have to result in synchronised biotic responses (Greenman and Benton, 2001; Currie, 2007). In fact, species abundance at a certain point in time depends on many factors: the actual climatic influence (mean and superimposed fluctuations), species sensitivities to climatic influences and previous abundance of the species itself and of other species.

Besides synchronised temporal fluctuations of model drivers, dispersal has been discussed as another important factor synchronising species abundances (e.g. Ripa, 2000; Liebhold et al., 2004; Bahn et al., 2008). The low degree of correlations in simulated species biomass among neighbouring single cells in simulations with SI extrapolation (Fig. 5a) and the strong similarities of biomass distributions among simulations with SC and SI drawn fluctuations in single cells over time (see ESM Fig. B.2) indicate that dispersal did not lead to a strong synchronising effect in the presented TreeMig simulations. On one hand, this might be due to the weak spatial linkage in TreeMig caused by a strong seed density regulation (see Lischke and Löffler, 2006) which diminishes the possible impact of large amounts of dispersed seeds. On the other hand, dispersal might be less important in synchronising plant abundances than in synchronising abundances of highly mobile taxa with low numbers of offspring, such as large animals (Bahn et al., 2008). Tree species, in particular, usually disperse by seeds, which subsequently are entirely subject to the local dynamics in the new environment.

Even though simulations with SC extrapolation did not show ubiquitous synchronism in species abundances, they showed partially synchronised species abundances. Comparisons between simulations with SC and SI extrapolation revealed greater synchronism in species abundances in simulations with SC extrapolation than in simulations with SI extrapolation (Fig. 5). In simulations with SI extrapolation nearly all climatically possible situations are experienced in one year, due to the large number (210×70) of transect cells with independently drawn bioclimatic fluctuations. Thus, applying the SI extrapolation method induced a

blurring effect, i.e. biomass maps simulated for all years and all repetitions with SI extrapolation look almost identical in the coarse view (Fig. 5). This blurring effect was particularly visible when summing the biomass over the entire transect. Simulations with SI extrapolation resulted in biomass sums that were nearly invariant over time and among repetitions for *O. carpinifolia* (Fig. 5). Large-scale fluctuations in the biomass that were observed in simulations with SC extrapolation – and are common in natural systems – were missing. This effect was also observed for the sum of the biomass of all simulated species (see ESM). The observed lack of variability can be explained via the central limit theorem (CLT), which states that sums of independent random variables will converge as long as they are not dominated by a small number of values (Spanos, 1999). The applicability of the CLT is supported by the fact that the moments of the biomass distribution over time are bounded and that the biomass in each cell is only a small fraction of the total. However, even in the SI simulations, biomass values in individual cells are not strictly independent variables, because of the underlying mean bioclimate (Fig. 1) and filter effects (Table 1), and because of the spatial linkage due to seed dispersal. Furthermore, the simulated biomass in each cell will be temporally correlated. Nevertheless, this lack of strict independence did not prevent convergence in the distributions of the transect sums in the SI simulations.

Overall, the results demonstrated that the SI method, which neglects spatial correlations in the bioclimatic fluctuations, led to a loss in the synchronisation of simulated tree species abundances.

4.2. Simulated tree species migration

Because of the large number of species parameters and interacting processes in TreeMig, no experiments were conducted in addition to the example setup. In order to enable a more detailed analysis, instead, a simple cellular automaton (CA) was developed. This CA abstracts from several processes and drivers represented in TreeMig. Each cell of the CA represents one individual (or cohort) which can be in one of three states. Thus, in contrast to TreeMig the CA has a discrete state space and the individuals do not have any attributes, such as fitness or height. Accordingly, there is no feedback between the environmental influences experienced by an individual and its contribution to future colonisations in the CA, which in TreeMig is realised via seed numbers proportional to tree heights (see Lischke et al., 2006). Due to this lack of the feedback in the CA, the number of required seed sources (s_{thresh}) is used as a proxy for propagule pressure, covering effects of species-specific differences in seed production.

Another important difference between the CA and TreeMig is that TreeMig simulations are driven by three bioclimate variables. These variables have different influences on the simulated processes and thus represent different filters (sensu Laakso et al., 2001) that can interfere with each other. The CA, in contrast, was only equipped with one environmental driver. The discrete nature of the CA, moreover, only allows for thresholds and not for other filter types. Whilst germination is implemented as a threshold in TreeMig, mortality only has a threshold effect if the population falls below a minimum density (see ESM A.3) and otherwise has a multiplicative thinning effect. The influence of the parameter m_{thresh} in CA simulations therefore might be too strong compared to mortality in TreeMig simulations. Finally, the simulation area used for TreeMig simulations has a high background heterogeneity in the bioclimate variables. As discussed in Section 4.1 this background heterogeneity can strongly influence species abundance, which in turn influences migration. In the CA simulations such background heterogeneity effects were neglected. In particular, we assumed that all cells in the CA were potentially inhabitable, and thus neglected potentially important effects caused by fragmentation (see e.g. Hof et al., 2011; Nabel et al., 2013).

Nevertheless, comparisons between simulations with the CA and with TreeMig demonstrate that observed trends in the northernmost occurrences simulated with TreeMig can be approximated by simulations with the CA (Fig. 6a and b compared to Fig. 7a and b). TreeMig simulations of the optimistic parameter set for *O. carpinifolia* showed nearly parallel trajectories outside of critical conditions. In CA simulations such behaviour would correspond to situations in which neither the threshold for required seed sources nor one of the environmental thresholds would be limiting (i.e. small values for the germination and the mortality threshold). In such cases, no big differences between SC and SI drawn environmental influences were observed (see e.g. the farthest left corner in the surface plots Fig. 8). To represent the migration outcomes of the moderate, less favourable parameter set for *O. carpinifolia*, more severe environmental thresholds were required in the CA simulations. This reflects the limitation by means of the bioclimate in the main bottleneck area in TreeMig simulations and the importance of interannual variability in the bioclimate in this area (see Nabel et al., 2013). The CA surface plots (e.g. Fig. 8) demonstrated this intuitive response to the applied environmental thresholds, which is consistent for the two extrapolation methods and throughout all applied parameter sets (for further surface plots see ESM).

Due to the small number of processes and in particular the small number of species parameters, the CA enabled a more detailed analysis of the influence of spatial correlation in the environmental fluctuations on migration. Simulations with the CA showed a broad range of possible migration outcomes for the different parameter sets (Fig. 7). Results of the CA demonstrate that simulations with the same parameter set can show different behaviour for SC and for SI drawn environmental influences. The tendency that SI-runs lead to faster migrations than SC-runs – as long as there is no strong positive density dependence – is intuitive. The environment in SC-runs only fluctuates among iterations but not among cells, i.e. the simulation area has a homogeneous environment in each iteration. Therefore, if the drawn environment falls below the mortality threshold in a SC-run, all cells in the juvenile state switch to the empty state, whilst mortality in SI-runs only affects single cells. Additionally, SC-runs only enable colonisation events in favourable iterations (exceeding the germination threshold). SI-runs, in contrast, potentially provide a colonisation option in each iteration as long as the number of seed sources is sufficiently high (exceeding the threshold for required seed sources), i.e. if propagule availability coincides with good conditions (cf. findings reviewed by Melbourne et al. (2007)). Whenever there is a strong positive density dependence, colonisation of a cell is dependent on the number of mature cells in the specified neighbourhood. In such cases, correlation in the environment is favourable, i.e. migration is faster in SC-runs, which is in agreement with the simulation results by McInerny et al. (2007). Overall, simulation results of the CA demonstrated that spatial correlations in the environmental driver can have promoting as well as inhibiting influences on the migration speed, depending on the simulated species traits. The two extrapolation methods can thus not simply be used interchangeably when simulating migration.

4.3. Methods to inter- and extrapolate bioclimate time series

In TreeMig simulations, spatially correlated (SC) fluctuations in the bioclimate driver were generated sampling uniformly from a base-year set and used for all cells of the simulation area. This method resembles the often applied method to cyclically repeat a set of base years (e.g. Hickler et al., 2012; Sato and Ise, 2012),

however, without the deterministically fixed temporal pattern. A fixed temporal pattern can lead to an incomplete or biased representation (Nabel et al., 2013), particularly in cases without a consistent signal of temporal autocorrelation, as in the current study (see ESM A.1.3).

The SC method was compared to a method generating spatially independent (SI) bioclimatic fluctuations, drawing each year and each cell uniformly from the empirical distributions found for single cells. Drawing directly from the empirical distributions is a simplification of drawing from derived probability distributions, which is the method originally suggested to be revisited in this study. This simplification was made in order to prevent effects of extreme values interfering with the effects of spatial correlation in the bioclimate driver. However, observed effects on the spatial arrangements of simulated species abundances will equally occur when drawing from derived probability distributions. In the CA simulations the environmental influence was again simplified and fluctuations were solely drawn from prescribed normal distributions with zero being the expected value. Using a normal distribution was motivated by the fact that (detrended) annual temperatures and derived bioclimate influences are often represented by normal distributions (Schär et al., 2004; Lischke et al., 2006). To obtain a spatial correlation in the driver of the CA simulations, only one pseudo-random number was drawn for the whole simulation area.

The results of this study demonstrated that drawing climatic fluctuations independently for single cells, and thus neglecting the spatial correlation of the fluctuations, led to severe differences in the spatial configuration of simulated tree species abundances. Furthermore, it also had an influence on tree species migration. It is thus not recommended to neglect the spatial correlation in the driver. However, the applied method to draw spatially correlated fluctuations also has drawbacks compared to the originally applied sampling from probability distributions. The main disadvantage is that only climatic patterns which are represented in the base-year set can actually occur in the generated time series (Bugmann, 2001). Thus, the length of the selected base period and the single selected base years could be influential. On one hand, when a series is too short or selected such that years with extreme values are not contained in the base period, no extreme events will occur in the generated time series. On the other hand, when years with extreme conditions are contained, then these will frequently be drawn (with a probability of 1/base period length). For the inter- and extrapolation of climate time series for simulations with spatially explicit and in particular spatially linked models it would thus be desirable to use more sophisticated methods. Ideally, a method should not neglect spatial correlation and the influence of the base period length and the selected base years should be small. One possibility could be to use statistically derived relationships of climatic fluctuations and static spatial properties to generate spatially correlated noise. One could, for example, use lapse-rates with elevation (as e.g. done by Schumacher et al., 2004 for temperature and precipitation). This approach is suitable for small areas, however, these relationships are not invariant on larger extents but vary, for example, with latitude and longitude (Jackson et al., 2009) and with distance to large water bodies (Hutchinson, 1995). Therefore, such a method can be rather data hungry and difficult to parametrise. For a detailed description of such methods see, for example, Hutchinson (1995).

5. Conclusions

Overall, the results demonstrated that neglecting the spatial correlations in climatic fluctuations for simulations with spatially explicit models can be a considerable interference because it can have a strong influence on the spatial arrangement of simulated species abundances and on migration outcomes.

The simulations with the illustrative example in TreeMig showed that neglecting the spatial correlation in climatic fluctuations might only be justifiable when one is solely interested in the mean abundance over an area and when abundance fluctuations do not matter. The observed invariance of the biomass sum over the transect area when neglecting the spatial correlation in bioclimatic fluctuations will also hold for other strongly climatically driven models because it is a consequence of the central limit theorem. For most applications drawing climatic fluctuations independently for single cells is therefore not recommended.

Simulations with the simple CA enabled a more detailed analysis of effects on simulated species migration and showed that the influence of spatial correlation in fluctuations of the environmental driver depends on species traits. Mostly, simulations with spatial correlation in environmental fluctuations resulted in slower migration rates than simulations without spatial correlation, however, it was opposite for species with strong positive density dependence. Simulations driven by environmental time series generated with a method which neglects spatial correlations should thus not even be used to estimate upper or lower limits of migration outcomes. They also should not be used to make comparisons among different species, at least not with models containing species parameters representing positive density dependence.

Acknowledgements

We like to thank David Gutzmann and an anonymous reviewer for their helpful comments, Thomas Wüst for the support with the cluster and Dirk Schmatz for assistance with the data preparation. Julia Nabel was partially funded by the Swiss National Science Foundation (SNF) Grant 315230-122434.

Appendices A–C. Supplementary Data

Supplementary data associated with this article can be found, in the online version, at http://dx.doi.org/10.1016/j.ecocom.2014.02.006.

References

Ahrens, J., Geveci, B., Law, C., 2005. ParaView: an end-user tool for large-data visualization. In: Hansen, C.D., Johnson, C.R. (Eds.), Visualization Handbook. Elsevier.

Bahn, V., Krohn, W.B., O'Connor, R.J., 2008. Dispersal leads to spatial autocorrelation in species distributions: a simulation model. Ecol. Model. 213, 285–292.

Breshears, D.D., Cobb, N.S., Rich, P.M., Price, K.P., Allen, C.D., Balice, R.G., Romme, W.H., Kastens, J.H., Floyd, M.L., Belnap, J., Anderson, J.J., Myers, O.B., Meyer, C.W., 2005. Regional vegetation die-off in response to global-change-type drought.In: Proc. Natl. Acad. Sci. USA, 102. pp. 15144–15148.

Brubaker, L.B., 1986. Responses of tree populations to climatic-change. Vegetatio 67, 119–130.

Bugmann, H., 2001. A review of forest gap models. Climatic Change 51, 259–305.

Currie, D.J., 2007. Disentangling the roles of environment and space in ecology. J. Biogeogr. 34, 2009–2011.

Epstein, H., Yu, Q., Kaplan, J., Lischke, H., 2007. Simulating future changes in arctic and subarctic vegetation. Comput. Sci. Eng. 9, 12–23.

Fischlin, A., Midgley, G.F., Price, J.T., Leemans, R., Gopal, B., Turley, C., Rounsevell, M.D.A., Dube, O.P., Tarazona, J., Velichko, A.A., 2007. Ecosystems, their properties, goods, and services. Climate Change 2007: Impacts, Adaptation and Vulnerability. Contribution of Working Group II to the Fourth Assessment Report of the Intergovernmental Panel on Climate Change. M.L. Parry, O.F. Canziani, J.P. Palutikof, P.J. van der Linden and C.E. Hanson (Eds.), Cambridge University Press, Cambridge, UK, pp. 211–272.

Giesecke, T., Miller, P.A., Sykes, M.T., Ojala, A.E.K., Seppä, H., Bradshaw, R.H.W., 2010. The effect of past changes in inter-annual temperature variability on tree distribution limits. J. Biogeogr. 37, 1394–1405.

Greenman, J.V., Benton, T.G., 2001. The impact of stochasticity on the behaviour of nonlinear population models: synchrony and the Moran effect. Oikos 93, 343–351.

Grenfell, B.T., Finkenstadt, B.F., Wilson, K., Coulson, T.N., Crawley, M., 2000. Reply: nonlinearity and the Moran effect. Nature 406,, 847–847.
Hickler, T., Vohland, K., Feehan, J., Miller, P.A., Smith, B., Costa, L., Giesecke, T., Fronzek, S., Carter, T.R., Cramer, W., Kühn, I., Sykes, M.T., 2012. Projecting the future distribution of European potential natural vegetation zones with a generalized, tree species-based dynamic vegetation model. Global Ecol. Biogeogr. 21, 50–63.
Hof, C., Levinsky, I., Araújo, M.B., Rahbek, C., 2011. Rethinking species' ability to cope with rapid climate change. Global Change Biol. 17, 2987–2990.
Hui, C., Krug, R.M., Richardson, D.M., 2011. Modelling spread in invasion ecology: a syntesis. In: Richardson, D.M. (Ed.), Fifty Years of Invasion Ecology. Wiley-Blackwell, UK, pp. 329–343.
Hutchinson, M., 1995. Stochastic space-time weather models from ground-based data. Agric. Forest Metorol. 73, 237–264.
Jackson, S.T., Betancourt, J.L., Booth, R.K., Gray, S.T., 2009. Ecology and the ratchet of events: climate variability, niche dimensions, and species distributions.In: Proc Natl. Acad. Sci. USA, 106. pp. 19685–19692.
Jarvis, A., Reuter, H., Nelson, A., Guevara, E., 2008. Hole-Filled SRTM for the Globe Version 4. Available from the CGIAR-CSI SRTM 90m Database. http://srtm.csi.cgiar.org.
Koenig, W., 2002. Global patterns of environmental synchrony and the Moran effect. Ecography 25, 283–288.
Koenig, W.D., Knops, J.M.H., 2013. Large-scale spatial synchrony and cross-synchrony in acorn production by two California oaks. Ecology 94, 83–93.
Laakso, J., Kaitala, V., Ranta, E., 2001. How does environmental variation translate into biological processes? Oikos 92, 119–122.
Liebhold, A., Koenig, W.D., Bjornstad, O.N., 2004. Spatial synchrony in population dynamics. Ann. Rev. Ecol. Evol. Syst. 35, 467–490.
Lischke, H., 2005. Modeling tree species migration in the Alps during the Holocene: what creates complexity? Ecol. Complex. 2, 159–174.
Lischke, H., von Grafenstein, U., Ammann, B., 2013. Forest dynamics during the transition from the Oldest Dryas to the Bølling-Allerød at Gerzensee – a simulation study. Palaeogeogr. Palaeoclimatol. Palaeoecol 391, 60–73.
Lischke, H., Löffler, T.J., 2006. Intra-specific density dependence is required to maintain species diversity in spatio-temporal forest simulations with reproduction. Ecol. Model. 198, 341–361.
Lischke, H., Zimmermann, N.E., Bolliger, J., Rickebusch, S., Löffler, T.J., 2006. TreeMig: a forest-landscape model for simulating spatio-temporal patterns from stand to landscape scale. Ecol. Model. 199, 409–420.
Lyford, M., Jackson, S., Betancourt, J., Gray, S., 2003. Influence of landscape structure and climate variability on a late Holocene plant migration. Ecol. Monogr. 73, 567–583.
McInerny, G., Travis, J.M.J., Dytham, C., 2007. Range shifting on a fragmented landscape. Ecol. Inform. 2, 1–8.
Melbourne, B.A., Cornell, H.V., Davies, K.F., Dugaw, C.J., Elmendorf, S., Freestone, A.L., Hall, R.J., Harrison, S., Hastings, A., Holland, M., Holyoak, M., Lambrinos, J., Moore, K., Yokomizo, H., 2007. Invasion in a heterogeneous world: resistance, coexistence or hostile takeover? Ecol. Lett. 10, 77–94.
Midgley, G.F., Thuiller, W., Higgins, S.I., 2007. Plant species migration as a key uncertainty in predicting future impacts of climate change on ecosystems: progress and challenges. In: Canadell, Josep G., Pataki, Diane E., Pitelka, Louis F. (Eds.), Terrestrial Ecosystems in a Changing World. Springer, Berlin Heidelberg, pp. 129–137.
Miller, P.A., Giesecke, T., Hickler, T., Bradshaw, R.H.W., Smith, B., Seppä, H., Valdes, P.J., Sykes, M.T., 2008. Exploring climatic and biotic controls on Holocene vegetation change in Fennoscandia. J. Ecol. 96, 247–259.
Nabel, J.E.M.S., Zurbriggen, N., Lischke, H., 2012. Impact of species parameter uncertainty in simulations of tree species migration with a spatially linked dynamic model. International Environmental Modelling and Software Society (iEMSs) 2012, Sixth Biennial Meeting, Leipzig, Germany, pp. 909–916. http://www.iemss.org/society/index.php/iemss-2012-proceedings.
Nabel, J.E.M.S., Zurbriggen, N., Lischke, H., 2013. Interannual climate variability and population density thresholds can have a substantial impact on simulated tree species' migration. Ecol. Model. 257, 88–100.
Normand, S., Ricklefs, R.E., Skov, F., Bladt, J., Tackenberg, O., Svenning, J.C., 2011. Postglacial migration supplements climate in determining plant species ranges in Europe. Proc. R. Soc. B: Biol. Sci. 278, 3644–4365.
Pearson, R.G., Dawson, T.P., 2003. Predicting the impacts of climate change on the distribution of species: are bioclimate envelope models useful? Global Ecol. Biogeogr. 12, 361–371.
Pitelka, L.F., Gardner, R.H., Ash, J., Berry, S., Gitay, H., Noble, I.R., Saunders, A., Bradshaw, R.H.W., Brubaker, L., Clark, J.S., Davis, M.B., Sugita, S., Dyer, J.M., Hengeveld, R., Hope, G., Huntley, B., King, G.A., Lavorel, S., Mack, R.N., Malanson, G.P., McGlone, M., Prentice, I.C., Rejmanek, M., 1997. Plant migration and climate change. Am. Sci. 85, 464–473.
Rickebusch, S., Lischke, H., Bugmann, H., Guisan, A., Zimmermann, N.E., 2007. Understanding the low-temperature limitations to forest growth through calibration of a forest dynamics model with tree-ring data. Forest Ecol. Manage. 246, 251–263.
Ripa, J., 2000. Analysing the Moran effect and dispersal: their significance and interaction in synchronous population dynamics. Oikos 89, 175–187.
Rosenzweig, C., Casassa, G., Karoly, D., Imeson, A., Liu, C., Menzel, A., Rawlins, S., Root, T., Seguin, B., Tryjanowski, P., 2007. Assessment of observed changes and responses in natural and managed systems. In: Parry, M.L., Canziani, O.F., Palutikof, J.P., van der Linden, P.J., Hanson, C.E. (Eds.), Impacts, Adaptation and Vulnerability. Contribution of Working Group II to the Fourth Assessment Report of the Intergovernmental Panel on Climate Change. Cambridge University Press, Cambridge, UK, pp. 79–131.
Sato, H., Ise, T., 2012. Effect of plant dynamic processes on African vegetation responses to climate change: analysis using the spatially explicit individual-based dynamic global vegetation model (SEIB-DGVM). J. Geophys. Res. – Biogeosci. 117, G03017.
Schär, C., Vidale, P.L., Lüthi, D., Frei, C., Haberli, C., Liniger, M.A., Appenzeller, C., 2004. The role of increasing temperature variability in European summer heatwaves. Nature 427, 332–336.
Schreiber, S.J., Ryan, M.E., 2011. Invasion speeds for structured populations in fluctuating environments. Theor. Ecol. 4, 423–434.
Schumacher, S., Bugmann, H., Mladenoff, D.J., 2004. Improving the formulation of tree growth and succession in a spatially explicit landscape model. Ecol. Model. 180, 175–194.
Spanos, A., 1999. Probability Theory and Statistical Inference: Econometric Modeling with Observational Data. Cambridge University Press.
van de Pol, M., Vindenes, Y., Sæther, B., Engen, S., Ens, B., Oosterbeek, K., Tinbergen, J., 2011. Poor environmental tracking can make extinction risk insensitive to the colour of environmental noise. Proc. R. Soc. B: Biol. Sci. 278, 3713–4372.
With, K.A., 2002. The landscape ecology of invasive spread. Conserv. Biol. 16, 1192–1203.